Journal of Food Bioactives
International Society for Nutraceuticals and Functional Foods
Original Research
J. Food Bioact. 2023;24:63–72

The enzymatic hydrolysates of *Andrias davidianus* mucus alleviates UVA-induced photoaging in the HSF cell and mouse skin

Li-Hua Zhou[a,b], Peng-Fei Zhang[c], Huan Zhang[d], Bei-Bei Dong[a,b], You-Nan Kou[a,b], Qing-Hua Luo[e], Ke-Guo Deng[f], Jun-Hua Zhuo[g], Heng-Yu Zheng[h], Wu-Yan Guo[i*] and Bo Zhang[j*]

[a]College of Pharmacy, Nankai University, Tianjin, 300350, China
[b]Tianjin Key Laboratory of Early Druggability Evaluation of Innovative Drugs, Tianjin International Joint Academy of Biomedicine, Tianjin, 300457, China
[c]Tianjin Pharmaceutical and Cosmetic Evaluation and Inspection Center, 300000, China
[d]Tianjin Key Laboratory of Industrial Microbiology, College of Biotechnology, Tianjin University of Science and Technology, Tianjin, P. R. 300457, China
[e]College of Biological and Environmental Engineering, Changsha University, Changsha, 410022, China
[f]College of Information Management and Engineering, Jishou University, Hunan, 416000, China
[g]Changsha Jinchi Biotechnology Co., LTD, Changsha, 410022, China
[h]Breast Disease Center, Peking University First Hospital, Beijing, 100084, China
[i]Tianjin JiAnKang Bio&TCM-technology Development Co., Ltd. Tianjin, 300457, China
[j]Tsinghua University Institute of TCM-X, Beijing, 100084, China
[*]**Corresponding author:** Bo Zhang, Tsinghua University Institute of TCM-X, Beijing, 100084, China. E-mail: zhangbo.2007@tsinghua.org.cn; Wu-Yan Guo, Tianjin JiAnKang Bio&TCM-technology Development Co., Ltd. Tianjin, 300457, China. E-mail: guowuyan213@126.com
DOI: 10.31665/JFB.2023.18365
Received: December 20, 2023; **Revised received & accepted:** December 28, 2023
Citation: Zhou, L.-H., Zhang, P.-F., Zhang, H., Dong, B.-B., Kou, Y.-N., Luo, Q.-H., Deng, K.-G., Zhuo, J.-H., Zheng, H.-Y., Guo, W.-Y., and Zhang, B. (2023). The enzymatic hydrolysates of *Andrias davidianus* mucus alleviates UVA-induced photoaging in the HSF cell and mouse skin. J. Food Bioact. 24: 63–72.

Abstract

Photoaging is the premature aging of skin caused by long-term exposure to ultraviolet radiation. The skin mucus of *Andrias davidianus* has anti-photoaging activity, but its active ingredients and mechanisms are not clear. In this study, we first investigated the photoprotective effect of enzymatic hydrolysates from *Andrias davidianus* mucus (AD-APRO) on UVA-irradiated responses in human skin fibroblasts (HSF) cells and mice. AD-APRO hindered the UVA induced activation of reactive oxygen species (ROS) and increased the activity of antioxidase in HSF cells. Furthermore, topical application of AD-APRO ameliorated skin photoaging in a mouse model by suppressing oxidative stress. CAMP and Peptide Ranker, two online tools, were used to predict the active peptides of AD-APRO against photoaging. The active peptides of AD-APRO were predicted to be KDACCNLVLHFNPRF, NLVLHFNPRF, FEWKP, and CNLVLHFNPRF. These results provide a basis for the study of the photoprotective effect of AD-APRO and suggest that it can be potentially used as an agent against UVA-induced skin photoaging in humans.

Keywords: *Andrias davidianus* mucus; Photoaging; UVA; Oxidative stress; Active peptides.

1. Introduction

Chronic exposure to UV irradiation causes premature skin aging (photoaging). Photoaged skin is characterized by loss of skin tone and resilience, increased roughness and dryness, irregular pigmentation, and deep wrinkles (Ansary et al., 2021). UV radiation con-

Copyright: © 2023 International Society for Nutraceuticals and Functional Foods.
All rights reserved.

sists of three components, UVA (320–400 nm), UVB (280–320 nm), and UVC (200–280 nm) (Sample and He, 2018). Whereas UVA and UVB reach the Earth in sufficient amounts to damage the skin, UVC is almost completely absorbed by the ozone layer (Strzalka et al., 2020). UVA penetrates deeper and can interact with fibroblasts (Battie et al., 2014). Exposing to UVA radiation can weaken skin defense mechanisms and degradate extracellular matrix, and ultimately lead to premature skin aging causing chronic skin inflammation (Ansary et al., 2021).

UVA causes photoaging via inducing collagenase in human dermal fibroblasts. Fibroblasts are the main source of collagen and matrix metalloproteinases (MMPs) (Jablonska et al., 2016), including MMP-1, MMP-3, and MMP-9. MMPs cause degradation of extracellular matrix (ECM) proteins such as collagen and elastin. Long-time exposure to UVA elevates the level of reactive oxygen species (ROS) like peroxide, superoxide anion, and singlet oxygen (Hseu et al., 2020). ROS induces many harmful effects including DNA damage, inflammatory reactions, and damage to ECM integrity (Saito et al., 2004).

Andrias davidianus, an endemic amphibian, is the longest-living and largest amphibian species in the world (Yang et al., 2017). The skin mucus of *Andrias davidianus* contains proteins, peptides, polysaccharides, and so on, which has antioxidant, anti-photoaging, and antibacterial activities. There are more than 155 kinds of proteins in the skin mucus of *Andrias davidianus* (Geng et al., 2015), some of which are involved in various physiological activities, including oxidation-reduction process, inflammatory response, extracellular matrix organization, cell-junction tissue, cytoskeletal organization, cell adhesion and so on (Geng et al., 2015). Recently, Deng et al. (2019) discovered that the skin mucus of *Andrias davidianus* had significantly stronger tissue adhesion, improved elasticity and biocompatibility, decreased skin wound healing time, and promoted wound regeneration and angiogenesis. In addition, Zhao et al. (2014) prepared oligopeptides of *Andrias davidianus* skin mucus as cosmetics to be used in 40 females suffering photoaging, which reduced wrinkles and delayed skin aging. The result prompted us to explore the potential of *Andrias davidianus* mucus in preventing UVA-induced skin damage.

This study was designed to verify the photoprotective effects of AD-APRO on UVA-induced photodamage in HSF cells *in vitro* and mouse models *in vivo*. Here, both *in vitro* and *in vivo* experimental results evidenced the anti-photoaging capacity of AD-APRO. According to proteomics study, the active peptides of AD-APRO against photoaging were speculated. Our findings define the cutaneoprotective roles of AD-APRO in UVA radiation and provide a molecular basis to alleviate and treat photodamaged skin.

2. Materials and methods

2.1. Materials

Andrias davidianus mucus was obtained from Xiangxi Salamander Chengjin Agricultural Science and Technology Co., Ltd. (Hunan, China). DPPH and ABTS were purchased from Beijing Solarbio Science and Technology Co., Ltd. (Beijing, China). Fetal bovine serum (FBS) was purchased from Invitrogen (Carlsbad, CA, USA). HSF cell line and DMEM/F12 medium was purchased from Saibaikang Biotechnology Co., LTD. (Shanghai, China). D-galactose, SOD, CAT, GPX, ROS, malondialdehyde (MDA) and hydroxyproline (HYP) ELISA Kits were purchased from Beijing Solarbio Science and Technology Co., Ltd. (Beijing, China).

2.2. Preparation of AD-APRO

Fifty grams of *Andrias davidianus* mucus was weighed, and acidic protease (E/S 0.5%) was added. Afterward, 100 mL ultrapure water was added and stirred. The pH of solution was adjusted to 3.0, digested at 35 °C for 3 h, and then inactivated at 60 °C for 10 min. Finally, the solution was adjusted to pH 7.0 and lyophilized.

2.3. DPPH and ABTS radical scavenging activities

ABTS and DPPH tests were performed on AD-APRO samples to determine antioxidant capacity. In order to determine the DPPH• and ABTS•+ scavenging ability, the following equation was used: DPPH or ABTS scavenging activity (%) = [A (free radical) − A (standard)]/A (free radical), where A is the absorbance value of DPPH at 517 nm or ABTS at 734 nm (Ryu et al., 2021). The results were independently repeated three times.

2.4. Cell culture

Human dermal fibroblast (HSF) cell line was obtained from Saibaikang Biotechnology Co., LTD. (Shanghai, China). Cells were maintained in a humidified atmosphere (95% air and 5% CO_2 at 37 °C) and were promulgated in DMEM/F12 supplemented with 15% heat-inactivated FBS, and 1% penicillin/streptomycin. Cultures were harvested and cell morphology was examined using an inverted microscope.

2.5. UVA irradiation and sample treatment

Before UVA irradiation, we pretreated cells with different concentrations of AD-APRO (0.1 μg/mL–1 μg/mL) for 24 h. Prior to incubation, PBS-washed cells were then resuspended in new phenol red-free DMEM/F12 containing 15% FBS. These cells were irradiated with 30 mL/cm^2 of UVA (λmax = 365 nm). After this incubation period, cells were fixed and or harvested to perform subsequent experiments in this study.

2.6. Cell proliferation assay

The CCK-8 colorimetric assay was used to measure cell viability. HSF cells (1×10^4 cells/well in a 96-well plate) were preincubated in the presence or absence of AD-APRO. This was then followed by irradiation along with UVA. After this, these irradiated and PBS washed cells were incubated with 100 μL of 10% CCK-8 in PBS for 2 h. The absorbance of color developed was measured at 450 nm using a microplate reader (Thermo, USA). Data were represented by the percentage of AD-APRO, which were compared to the control cells and randomly assigned a viability value of 100%.

2.7. β-galactosidase staining

Cells (1×10^5 cells/well in a 12-well plate) of each group were seeded in medium. Cells were stained according to the kit instructions. After overnight incubation, stained cells were observed under a microscope.

Table 1. Dose of administration in mice model induced by UVA combined with D-gal

Group	UVA radiation dose ($J/cm^2/d$)	1% D-gal injection dose (mL/d)	Dose of drug application (mL/d)
Control	0	0	0
Model	10	0.2	0
VC	10	0.2	0.2
L (150 mg/mL AD-APRO)	10	0.2	0.2
H (450 mg/mL AD-APRO)	10	0.2	0.2

2.8. Determination of ROS

HSF cells were pretreated with different concentrations of AD-APRO and then exposed to UVA irradiation. The cellular ROS was quantified using an ROS assay kit.

2.9. Measurement of SOD, CAT, GPX, and MDA

HSF cells were harvested and disrupted with a cell disrupter (Constant Systems). Then the lysed cells were centrifuged at 12,000 g for 10 min at 4°C to obtain the supernatant. The contents of SOD, CAT, GPX, and MDA were detected by kits according to the manufacturer's protocols.

2.10. Animal study

Female Kunming mice (8-week-old, 30–35 g) were purchased from Tianjin International Joint Academy of Biomedicine (Tianjin, China). Mice were housed 5 per cage, allowed to access food and water freely, and maintained at a constant temperature (23 ± 1 °C) and humidity (55 ± 5%) under a 12 h light/dark cycle. The investigation conformed to the International Guiding Principles for Biomedical Research Involving Animals (1985). All experimental procedures were conducted and performed as the policies for animal care and use encompass regulations approved by the Institutional Animal Care and Use Committee of Nankai University. The mice were randomly divided into five groups (10 mice in one group) and processed using the following protocol (Table 1):

2.11. Measurement of SOD, CAT, MDA, and HYP in mice skin

Approximately 0.1 g of skin tissue was collected and grinded. Then the tissue was lysed using RIPA buffer on ice. According to the kit instructions, the SOD, CAT, MDA, and HYP contents of tissue supernatant were determined using.

2.12. Proteomics study

Skin was lysed in 1% Triton X-100, 1% protease inhibitor, centrifuged at 4 °C at 12,000 g for 10 min. The supernatant of skin was added with trypsin for 24 h and 5 mM dithiothreitol (DTT) for 30 min. Protein determination was performed with BCA assay. The peptides were separated using an EASY-nLC 1200 UPLC Chromatography System. Peptides were eluted with a gradient of mobile phases A and B. Mobile phase A contained 2% acetonitrile and 0.1% formic acid in water, and mobile phase B was composed of 90% acetonitrile and 0.1% formic acid in water. The gradient conditions were as follows: 6–23% B for 68 min, 23–32% B for 14 min, 32–80% B for 4 min, 80% B for 4 min at a flow rate of 500 nL/min. The peptides were separated by an UPLC Chromatography System and then entered the Orbitrap Exploris™ 480 mass spectrometer for analysis.

Data were processed with Proteome Discoverer v2.4.1.15 and searched against the Mus_musculus_10090_SP_20220107.fasta. All data was searched as a single batch and the peptide spectral matches (PSMs) of each database search filtered to 1% FDR using a target/decoy approach with percolator. The identified proteins were functionally annotated, including the Gene Ontology (GO), KEGG pathways, and subcellular structural localization.

2.13. Prediction of active peptides in AD-APRO

Peptides were eluted with a gradient of mobile phases A and B. Mobile phase A contained 2% acetonitrile and 0.1% formic acid in water, and mobile phase B was composed of 80% acetonitrile and 0.1% formic acid in water. The gradient conditions were as follows: 5–23% B for 56 min, 23–29% B for 6 min, 29–38% B for 1 min, 38–100% B for 27 min at a flow rate of 300 nL/min. Data acquisition software was Thermo Xcalibur 4.0.

Online tools were used to screen the identified peptides of AD-APRO and take the intersection from all results. On the one hand, peptide sequences were input into the Peptide Ranker (http://distilldeep.ucd.ie/PeptideRanker/) for evaluation. On the other hand, the information about peptides of AD-APRO and the target protein were input into the CAMP (https://github.com/twopin/CAMP) to screen the most active peptides according to the binding action score (Lei et al., 2021).

2.14. Statistical analysis

All experimental statistical calculations of the one-way analysis of variance (one-way ANOVA) were performed using GraphPad Prism 9.0 software. The experimental results are presented as the means ± standard deviation, and p value < 0.05 indicates significance.

3. Results

3.1. Characterization of AD-APRO

In the UV spectrum, the absorption peak at 205 and 214 nm indicated that AD-APRO might contain carboxyl and amide groups (Figure 1a). From the IR spectrum, AD-APRO exhibited absorption bands due to the presence of amide (3,287.78, 1,649.43, and 1,449.63 cm^{-1}) and hydroxyl groups (2,961.05 and 1,393.22 cm^{-1})

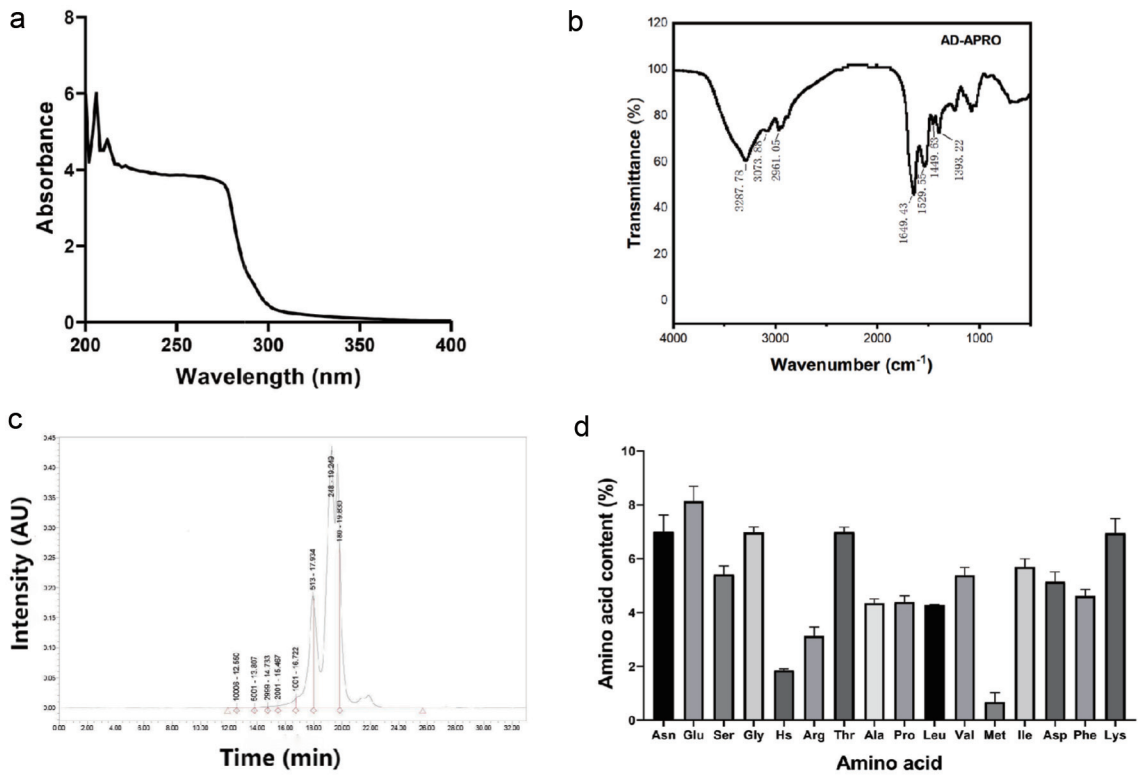


Figure 1. Characteristic of AD-APRO. (a) UV spectrum. (b) IR spectrum. (c) Gel Permeation Chromatography (GPC). (d) Animo acid.

(Figure 1b). The molecular weight distribution of AD-APRO was determined by gel permeation chromatography (GPC). The results demonstrated that AD-APRO was mainly containing short peptides with molecular weights below 1,000 Da (Figure 1c). In addition, AD-APRO contained multiple amino acids, including glutamate, lysine, threonine, glycine, asparagine, valine, and so on (Figure 1d). These results indicated that AD-APRO consisted of small molecular weight peptide, which is easy to be absorbed by the skin.

3.2. Antioxidant activity of AD-APRO in vitro

DPPH radical and ABTS radical experiments were used to explore the antioxidant activity of AD-APRO. Through the analysis of radical scavenging rate, the EC_{50} values of AD-APRO against DPPH and ABTS radicals were 78.48 μg/mL and 2.077 mg/mL (Figure 2). AD-APRO showed great DPPH radical scavenging activity at low concentrations and the DPPH radical scavenging rates at five concentrations presented a dose-dependent trend, thus AD-APRO demonstrating good antioxidant activity.

3.3. AD-APRO alleviates UVA-induced cell photodamage in HSF

HSF cells are normally spindle-shaped with a regular oval nucleus. Cell morphology at different radiation doses was microscopically examined. Results showed the HSF proliferation activity in the 0, 15, 30, and 45 mL/cm^2 dose groups decreased gradually with the increase of UVA radiation dose (Figure 3a). The CCK-8 cell viability assay confirmed the above observations that the viability

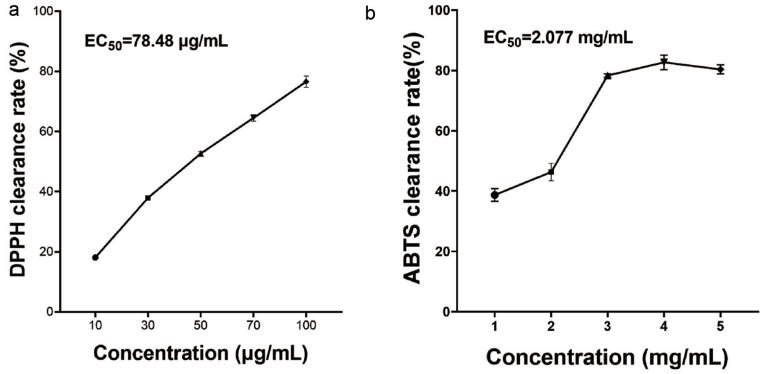


Figure 2. Antioxidant activity of AD-APRO *in vitro*. (a) DPPH radical scavenging rate of AD-APRO. (b) ABTS radical scavenging rate of AD-APRO.

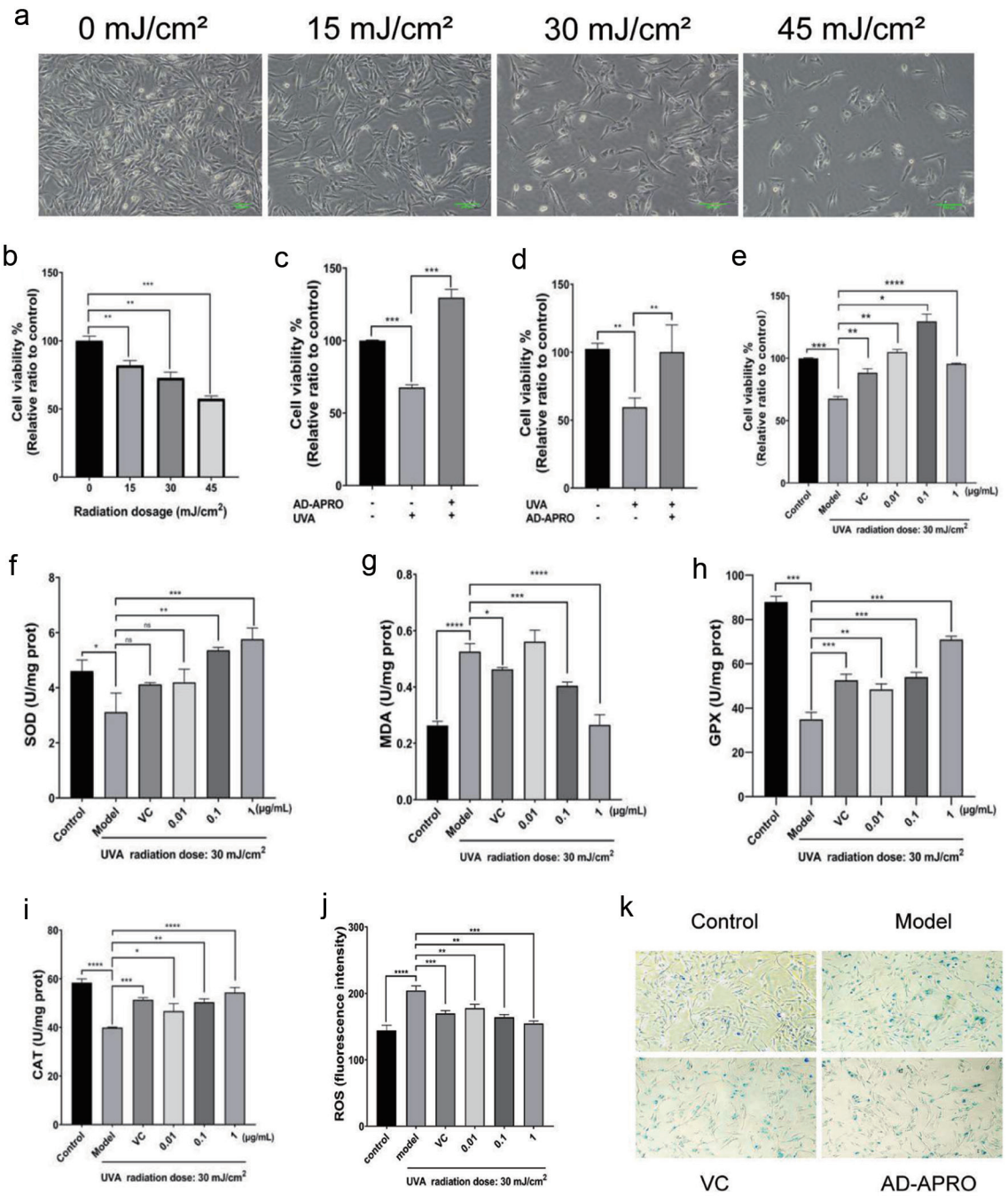


Figure 3. AD-APRO alleviates the damage of HSF cells caused by photoaging. (a) Cell morphology. (b–e) Cell viability. (f–j) Activity and content of SOD, MDA, GPX, CAT. (k) β-Gal staining.

of HSF was negatively correlated with the radiation dose (Figure 3b). Next, the order of photoaging and dosing was investigated. Compared with the model group, the HSF viability of preapplication of AD-APRO group was 129.5 ± 5.773% (Figure 3c). While AD-APRO was administered after 30 mL/cm^2 at UVA exposure, the viability of HSF exhibited less cell viability (100.2 ± 19.93%) (Figure 3d). The pre-application of AD-APRO demonstrated a significant anti-photoaging effect. All three concentrations of AD-APRO (0.01, 0.1, and 1 μg/mL) significantly increased cell viability in HSF compared to the model group (Figure 3e).

To understand the underlying mechanisms, we investigated if AD-APRO exerted its anti-photoaging effect via antioxidation. The activity of key antioxidant enzymes including CAT, SOD, and GPX as well as MDA content and ROS activity were determined. The results showed that AD-APRO treatment enhanced the activity of antioxidative enzymes in HSF cells. In addition, the level of ROS and MDA were suppressed after AD-APRO treatment (Figure 3f-j). This suggested that AD-APRO could exert anti-photoag-

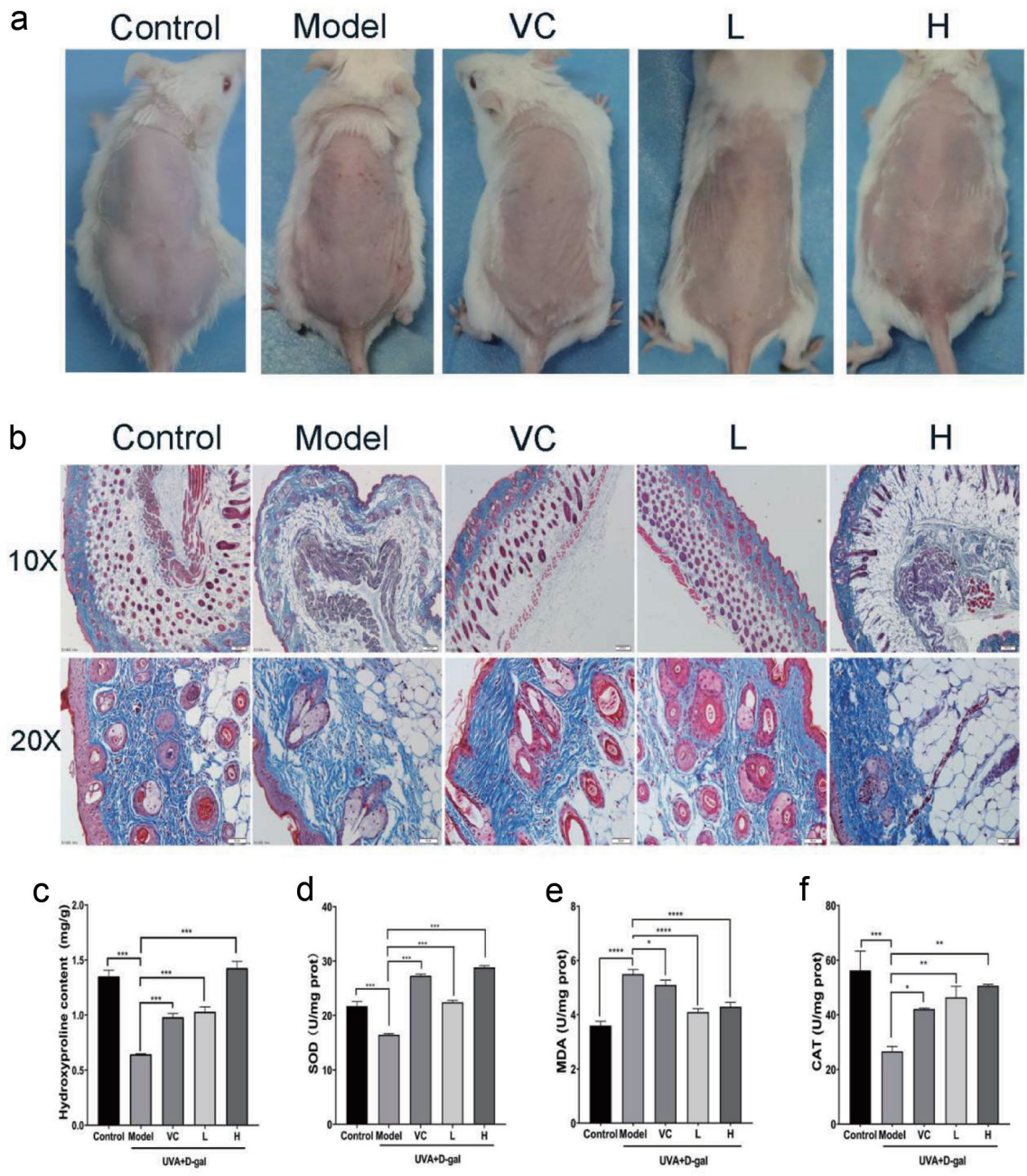


Figure 4. The effect of AD-APRO on mouse skin aging induced by UVA combined with D-galactose. (a) The surface examination of dorsal skin. (b) MASOON staining of skin tissue. (c–f) Measurement of HYP, SOD, MDA, CAT.

ing effect via inhibition of oxidative stress.

The increased activity of senescence-associated β-galactosidase (SA-β-gal) is commonly used as a marker of cellular senescence. X-Gal, as a substrate, is catalyzed by SA-β-gal to generate dark blue products, which colours senescent cells blue and can be viewed directly visualized by microscopy. The proportion of blue cells in the AD-APRO treatment group was significantly decreased compared with the model group, indicating that AD-APRO could inhibit the generation of senescent cells (Figure 3k). Thus, the AD-APRO application prior to irradiation protects the HSF cells from UVA-induced photodamage.

3.4. AD-APRO alleviates photoaging induced by UVA combined with D-galactose in mouse skin

In order to further evaluate the anti-photoaging activity of AD-APRO, photoaging models of UVA combined with D-galactose induction were established. UVA irradiation caused obvious erythema and wrinkles as well as severe dryness on the dorsal skin of the mice, compared with the normal control group. However, these symptoms were eased by the transdermal application of AD-APRO and VC (Figure 4a). Histological analysis of the model

group revealed disordered collagen fiber after UVA irradiation. Compared with the model group, the AD-APRO-treated groups showed the following significant improvements: a reduction in epidermal thickness on the dorsal skin, cell shape in the epidermal layer was more regular, and not shrunken. Beyond that, collagen fiber density in the dermis with AD-APRO treated increased significantly (Figure 4b). This data indicated that AD-APRO has the ability to protect mouse skin from UVA radiation.

The anti-photoaging effect of AD-APRO was further evaluated by measuring the hydroxyproline (HYP) content and antioxidant activity in mouse skin. Hydroxyproline, a major component of collagen, can reflect the status of skin indirectly. The content of HYP was depressed in the model group mice, compared with that in the normal control group but was expressed at much higher levels following the application of AD-APRO and VC (Figure 4c). The results showed that AD-APRO treatment enhanced the activity of antioxidative enzymes in mouse skin tissues. In addition, the level of MDA was suppressed after AD-APRO treatment (Figure 4d–f).

3.5. Proteomics research

Based on the above experiments, we learned that AD-APRO delayed skin photoaging by inhibiting oxidative stress. We performed proteomic studies on mouse skin tissues to deeply elucidate the mechanism of anti-photoaging of AD-APRO. There were 205 proteins between the AD-APRO and Model groups, with 77 upregulated and 128 downregulated (Figure 5a–b). GO analysis found that the differently expressed proteins were mainly located in intracellular and protein complexes, with antioxidant, catalytic, and molecular function regulators, and involved in biological processes such as cellular processes, biological regulation, stimulus response, metabolic processes, and immune system processes (Figure 5d–f). KEGG enrichment analysis showed a total of 17 pathways involved, and it is speculated that AD-APRO delay of aging in mice may be related to signaling pathways such as complement and coagulation cascade, cholesterol metabolism, lipid and atherosclerosis and so on (Figure 5g). By interaction analysis of proteins, the top 10 differently expressed proteins were selected according to the size of degree value (Figure 5c), where Complement C3 (C3) could induce MMPs and ROS to generate, and Fibronectin1 (Fn1) promoted the expression and secretion of collagen. Therefore, it is speculated that C3 and Fn1 may be the key targets of AD-APRO against photoaging.

3.6. Prediction of active peptides in AD-APRO

Two key targets were obtained to inform the selection of targets in active peptides prediction according to proteomics studies. Based on the two evaluation methods of Peptide Ranker and CAMP, the active peptides is KDACCNLVLHFNPRF, NLVLHFNPRF, CNLVLHFNPRF and FEWKP according to the high activity prediction score and the binding strength to the target (Figure 6). It was found that the position of amino acids in the peptides affected their biological activity (Li and Li, 2013), and the antioxidant activity was high when the peptides contained hydrophobic (Leu, Val, and Gly) and aromatic amino acids (Phe and Tyr).

4. Discussion

UVA penetrates deep into the skin and damages the dermal compartment leading to wrinkles, photoaging, and even skin cancer (Shen et al., 2014). Photoprotective agents and measures aimed at reducing tun exposure and preventing the development of acute and chronic actinic damage are highly recommended by dermatologists (Hao et al., 2019). The presence of antioxidant peptides in amphibian skin secretions has contributed much to the study of antiaging pharmaceuticals (Placido et al., 2020). It's reported that *Andrias davidianus* is a unique amphibian in China, which of skin mucus has anti-photoaging effects in clinical studies (Zhao et al., 2014). Thus, it would be interesting if the active peptide of *Andrias davidianus* skin mucus could be proved to act as a photoprotective reagent against UVA.

In the present study, the enzymatic hydrolysate from *Andrias davidianus* mucus (AD-APRO) was first evaluated as a potential therapeutic agent for photoaging cells and skin. Previous studies have found that the antioxidant activity of peptides can depend on their amino acid composition, active amino acid position, and molecular mass. Generally, polypeptides with low molecular weight showed stronger antioxidant and anti-photoaging activities (Kim et al., 2018; Kim et al., 2022). AD-APRO was found that its molecular weight was mainly concentrated in the range of 100–1,000 Da. Amino acids have certain antioxidant activity (Liu et al., 2021), and it is found that tyrosine, valine, histidine, arginine, phenylalanine, lysine, and methionine can clear the ABTS radical. The study showed that AD-APRO contains the above amino acids. The good antioxidant activity of AD-APRO *in vitro* was confirmed by the radical scavenging rate. Oxidative stress, caused by excessive production of free radicals, is the starting point of skin photodamage. Thus, we have speculated that AD-APRO might have anti-photoaging activity in skin.

The typical characteristics of skin photoaging include wrinkling, sagging, and loss of elasticity, which primarily depends on the level of collagen synthesized by fibroblasts (HSF) (Weihermann et al., 2021; Mehta., 2016). Thus, HSF is an ideal cell model for the study of skin photoaging. In this study, we investigated the protective effects of AD-APRO on HSF cells in UVA-induced oxidative stress. Significant change in cell survival was observed after UVA irradiation, the cell survival was reduced to 67.6% compared with control after 30 mL/cm^2 UVA irradiation. Cell viability was determined using CCK-8 assays and showed that pretreatment with AD-APRO alleviated the toxic effect of UVA on HSF cells. SA-β-galactosidase activity, a hallmark of cellular senescence (Biran et al., 2017), was significantly decreased after pretreatment with AD-APRO compared with the model group. It is well known that a detrimental foreign stimulus can induce the abnormal accumulation of ROS. ROS can attack liposomes in skin cells to produce MDA, an important product of lipid peroxidation (Gawel et al., 2004; Su et al., 2019). MDA makes macromolecular cross-linking (Su et al., 2019). MDA makes macromolecular cross-linking of skin tissue and damages dermal tissue (Maitz et al., 2020). Antioxidant enzymes, including SOD, CAT, and GPX can scavenge the excessive ROS to maintain the balance of redox state. In effect, the increased ROS excessive production and oxidative stress is accompanied by the decrease of antioxidant enzyme activity. Studies showed that ROS and MDA significantly increased, and the activity of antioxidant enzymes significantly decreased after UVA exposure. While these effects could be ameliorated by pretreatment of HSF cells with AD-APRO. AD-APRO might exert an anti-photoaging role by improving antioxidant activity.

In order to better simulate the generation of skin aging and evaluate the anti-photoaging effect of AD-APRO, a subacute aging mouse model by UVA combined with D-galactose induction was established. Photographs of the dorsal skin were obtained after 6 weeks of AD-APRO. Erythemas and wrinkles appeared on the skin of the non-AD-APRO treated mice. Moreover, the expression

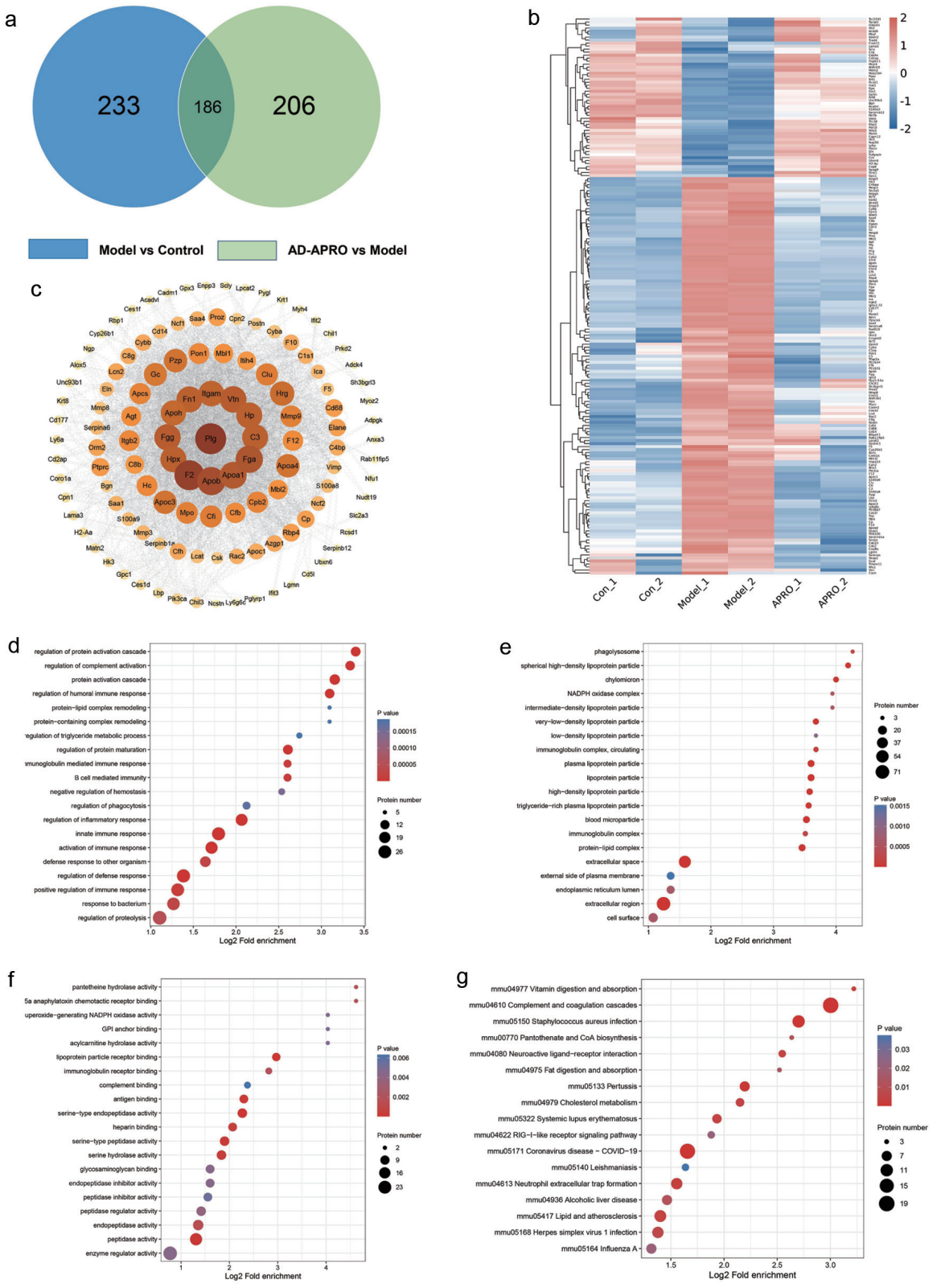


Figure 5. Peptide prediction of anti-photoaging activity in AD-APRO. (a) VENN diagram. (b) Heatmap. (c) Interaction map of the differently expressed proteins. (d–f) GO functional analysis and KEGG pathway enrichment analysis. (d) The top 20 BP terms. (e) The top of 20 CC terms. (f) The top 20 MF terms. (g) The KEGG enrichment analysis.

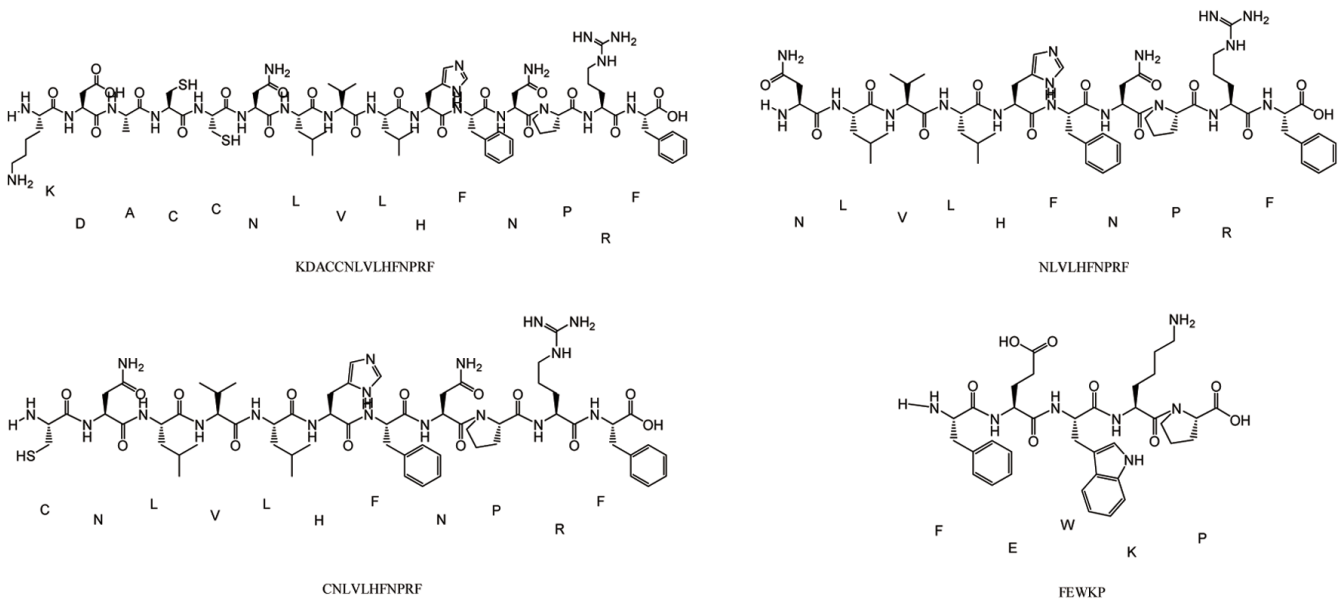


Figure 6. Structure of active peptides in AD-APRO.

of collagen fibers in mouse skin was evaluated by Masson's trichrome staining. More disordered collagen fibers were observed in the model group mice. Strikingly, these above symptoms were improved following the transdermal application of AD-APRO. Hydroxyproline (HYP), a major amino acid in collagen, plays an essential role in fiber stability (Zhuang and Lyga, 2014). The result showed that AD-APRO pretreatment significantly inhibited the decrease of HYP caused by UV radiation. The antioxidant effects of AD-APRO were demonstrated by changes in the levels of CAT, SOD, and MDA. On the whole, the application of AD-APRO protected mouse skin against UVA-induced photoaging. Finally, a proteomic profile was performed on mouse skin to further elucidate the putative mechanism of action of AD-APRO against photoaging. A total of 185 differentially expressed proteins were detected using label free quantification method. By analysis of protein network interaction of differential proteins, we speculated Fn1 and C3 might be critical targets of AD-APRO against skin photoaging. Of these, C3 could induce the generation of MMPs and ROS (Rauterberg., et al; Kim et al., 2022). Fn1 could promote the expression and secretion of collagen, thereby reducing wrinkle (Kim et al., 2022). The active peptide of AD-APRO against photoaging was predicted by Peptide Ranker and CAMP. According to the binding strength and activity of target and peptide sequences, KDACCNLVLHFNPRF, NLVLHFNPRF, CNLVLHFNPRF, and FEWKP may be the key active peptides. It was found that the biological activity of peptides depended mainly on their amino acid composition and sequence (Lei et al., 2021). Peptides with a high proportion of hydrophobic and aromatic amino acids frequently exhibit high antioxidant activity, such as Leu, Val, Phe, and Tyr (Li et al., 2011). All four predicted peptides matched the criterion, indicating that AD-APRO may have anti-photoaging activity due to these peptides.

Altogether, our study opens a promising way to explain the antiphotoaging of AD-APRO and provides an innovative method to predict active peptides. The potential anti-photoaging effect of AD-APRO demonstrated in our animal assays provides good support for further transformation of the products, with the overall aim of achieving younger and healthier skin.

Acknowledgments

We would like to thank Jishou University for funding support.

Data availability statement

All data generated or analyzed during this study are included in this article. Further enquiries can be directed to the corresponding author.

Funding

This research was funded by China Postdoctoral Science Foundation (2020T130093ZX) and Open Project of Hunan Provincial Engineering Laboratory for Conservation and Comprehensive Utilization of Giant Salamander Resources (DNOC2101).

Conflict of interest

All authors reveal no conflict of interest in this study.

References

Ansary, T.M., Hossain, M.R., Kamiya, K., Komine, M., and Ohtsuki, M. (2021). Inflammatory Molecules Associated with Ultraviolet Radiation-Mediated Skin Aging. Int. J. Mol. Sci. 22(8): 3974.

Battie, C., Jitsukawa, S., Bernerd, F., Del Bino, S., Marionnet, C., and Verschoore, M. (2014). New insights in photoaging, UVA induced damage and skin types. Exp. Dermatol. 23(Suppl 1): 7–12.

Biran, A., Zada, L., Abou Karam, P., Vadai, E., Roitman, L., Ovadya, Y., Porat, Z., and Krizhanovsky, V. (2017). Quantitative identification of senescent cells in aging and disease. Aging cell 16(4): 661–671.

Gaweł, S., Wardas, M., Niedworok, E., and Wardas, P. (2004). Dialdehyd malonowy (MDA) jako wskaźnik procesów peroksydacji lipidów w

organizmie [Malondialdehyde (MDA) as a lipid peroxidation marker]. Wiad. Lek. (Warsaw, Poland) 57(9-10): 453–455.

Geng, X., Wei, H., Shang, H., Zhou, M., Chen, B., Zhang, F., Zang, X., Li, P., Sun, J., Che, J., Zhang, Y., and Xu, C. (2015). Proteomic analysis of the skin of Chinese giant salamander (Andrias davidianus). J. Proteomics 119: 196–208.

Hao, D., Wen, X., Liu, L., Wang, L., Zhou, X., Li, Y., Zeng, X., He, G., and Jiang, X. (2019). Sanshool improves UVB-induced skin photodamage by targeting JAK2/STAT3-dependent autophagy. Cell Death Dis. 10(1): 19.

Hseu, Y.C., Vudhya Gowrisankar, Y., Chen, X.Z., Yang, Y.C., and Yang, H.L. (2020). The Antiaging Activity of Ergothioneine in UVA-Irradiated Human Dermal Fibroblasts via the Inhibition of the AP-1 Pathway and the Activation of Nrf2-Mediated Antioxidant Genes. Oxid. Med. Cell. Longevity 2020: 2576823.

Jabłońska-Trypuć, A., Matejczyk, M., and Rosochacki, S. (2016). Matrix metalloproteinases (MMPs), the main extracellular matrix (ECM) enzymes in collagen degradation, as a target for anticancer drugs. J. Enzyme Inhib. Med. Chem. 31(sup1): 177–183.

Kim, D.U., Chung, H.C., Choi, J., Sakai, Y., and Lee, B.Y. (2018). Oral Intake of Low-Molecular-Weight Collagen Peptide Improves Hydration, Elasticity, and Wrinkling in Human Skin: A Randomized, Double-Blind, Placebo-Controlled Study. Nutrients 10(7): 826.

Kim, D., Lee, M., Yang, J.H., Yang, J.S., and Kim, O.K. (2022). Dual Skin-Whitening and Anti-wrinkle Function of Low-Molecular-Weight Fish Collagen. J. Med. Food 25(2): 192–204.

Kim, S.H., Kim, J.H., Lee, S.J., Jung, M.S., Jeong, D.H., and Lee, K.H. (2022). Minimally invasive skin sampling and transcriptome analysis using microneedles for skin type biomarker research. Sking Res. Technol. 28(2): 322–335.

Langrock, T., and Hoffmann, R. (2019). Analysis of Hydroxyproline in Collagen Hydrolysates. Methods Mol. Biol. (Clifton, N.J.) 2030: 47–56.

Lei, Y., Li, S., Liu, Z., Wan, F., Tian, T., Li, S., Zhao, D., and Zeng, J. (2021). A deep-learning framework for multi-level peptide-protein interaction prediction. Nat. Commun. 12(1): 5465.

Li, Y.W., and Li, B. (2013). Characterization of structure-antioxidant activity relationship of peptides in free radical systems using QSAR models: key sequence positions and their amino acid properties. J. Theor. Biol. 318: 29–43.

Li, Y.X., Shao, Y.H., and Deng, N.Y. (2011). Improved prediction of palmitoylation sites using PWMs and SVM. Protein Pept. Lett. 18(2): 186–193.

Liu, W.Y., Zhang, J.T., Miyakawa, T., Li, G.M., Gu, R.Z., and Tanokura, M. (2021). Antioxidant properties and inhibition of angiotensin-converting enzyme by highly active peptides from wheat gluten. Sci. Rep. 11(1): 5206.

Maitz, J., Wang, Y., Fathi, A., Ximena Escobar, F., Parungao, R., van Zuijlen, P., Maitz, P., and Li, Z. (2020). The effects of cross-linking a collagen-elastin dermal template on scaffold bio-stability and degradation. J. Tissue Eng. Regener. Med. 14(9): 1189–1200.

Mehta-Ambalal, S.R. (2016). Neocollagenesis and Neoelastinogenesis: From the Laboratory to the Clinic. J. Cutan. Aesthet. Surg. 9(3): 145–151.

Plácido, A., Bueno, J., Barbosa, E.A., Moreira, D.C., Dias, J.D.N., Cabral, W.F., Albuquerque, P., Bessa, L.J., Freitas, J., Kuckelhaus, S.A.S., Lima, F.C.D.A., Batagin-Neto, A., Brand, G.D., Relvas, J.B., Leite, J.R.S.A., and Eaton, P. (2020). The Antioxidant Peptide Salamandrin-I: First Bioactive Peptide Identified from Skin Secretion of Salamandra Genus (Salamandra salamandra). Biomolecules 10(4): 512.

Rauterberg, A., Jung, E.G., and Rauterberg, E.W. (1993). Complement deposits in epidermal cells after ultraviolet B exposure. Photodermatol., Photoimmunol. Photomed. 9(4): 135–143.

Ryu, S.M., Nam, H.H., Kim, J.S., Song, J.H., Seo, Y.H., Kim, H.S., Lee, A.Y., Kim, W.J., Lee, D., Moon, B.C., and Lee, J. (2021). Chemical constituents of the egg cases of tenodera angustipennis (Mantidis ootheca) with intracellular reactive oxygen species scavenging activity. Biomolecules 11(4): 556.

Saito, Y., Shiga, A., Yoshida, Y., Furuhashi, T., Fujita, Y., and Niki, E. (2004). Effects of a novel gaseous antioxidative system containing a rosemary extract on the oxidation induced by nitrogen dioxide and ultraviolet radiation. Biosci., Biotechnol., Biochem. 68(4): 781–786.

Sample, A., and He, Y.Y. (2018). Mechanisms and prevention of UV-induced melanoma. Photodermatol., Photoimmunol. Photomed. 34(1): 13–24.

Seite, S., Zucchi, H., Septier, D., Igondjo-Tchen, S., Senni, K., and Godeau, G. (2006). Elastin changes during chronological and photo-ageing: the important role of lysozyme. J. Eur. Acad. Dermatol. Venereol. 20(8): 980–987.

Shen, C., Turney, T.W., Piva, T.J., Feltis, B.N., and Wright, P.F. (2014). Comparison of UVA-induced ROS and sunscreen nanoparticle-generated ROS in human immune cells. Photochem. Photobiol. Sci. 13(5): 781–788.

Strzałka, W., Zgłobicki, P., Kowalska, E., Bażant, A., Dziga, D., and Banaś, A.K. (2020). The Dark Side of UV-Induced DNA Lesion Repair. Genes 11(12): 1450.

Su, L.J., Zhang, J.H., Gomez, H., Murugan, R., Hong, X., Xu, D., Jiang, F., and Peng, Z.Y. (2019). Reactive Oxygen Species-Induced Lipid Peroxidation in Apoptosis, Autophagy, and Ferroptosis. Oxid. Med. Cell. Longevity 2019: 5080843.

Yang, H., Liu, R., Cui, D., Liu, H., Xiong, D., Liu, X., and Wang, L. (2017). Analysis on the expression and function of a chicken-type and goose-type lysozymes in Chinese giant salamanders Andrias davidianus. Dev. Comp. Immunol. 72: 69–78.

Zhang, X., Jiang, L., Li, X., Zheng, L., Dang, R., Liu, X., Wang, X., Chen, L., Zhang, Y.S., Zhang, J., and Yang, D. (2022). A Bioinspired Hemostatic Powder Derived from the Skin Secretion of Andrias davidianus for Rapid Hemostasis and Intraoral Wound Healing. Small (Weinheim an der Bergstrasse, Germany) 18(3): e2101699.

Zhao, X.Z., Wei, N., Zhang, L.Z., Zhou, M., and Guo, J. (2014). Clinical study of anti-skin photoaging on the oligosaccharide peptides of Andrias davidianus. Med. Beauty in China 4(03): 78–80.

Zhuang, Y., and Lyga, J. (2014). Inflammaging in skin and other tissues - the roles of complement system and macrophage. Inflammation Allergy: Drug Targets 13(3): 153–161.